Supplementary Information

Title:

TGF-β Signaling Regulates Neuronal C1q Expression and Developmental Synaptic Refinement

Authors:

Allison R. Bialas and Beth Stevens

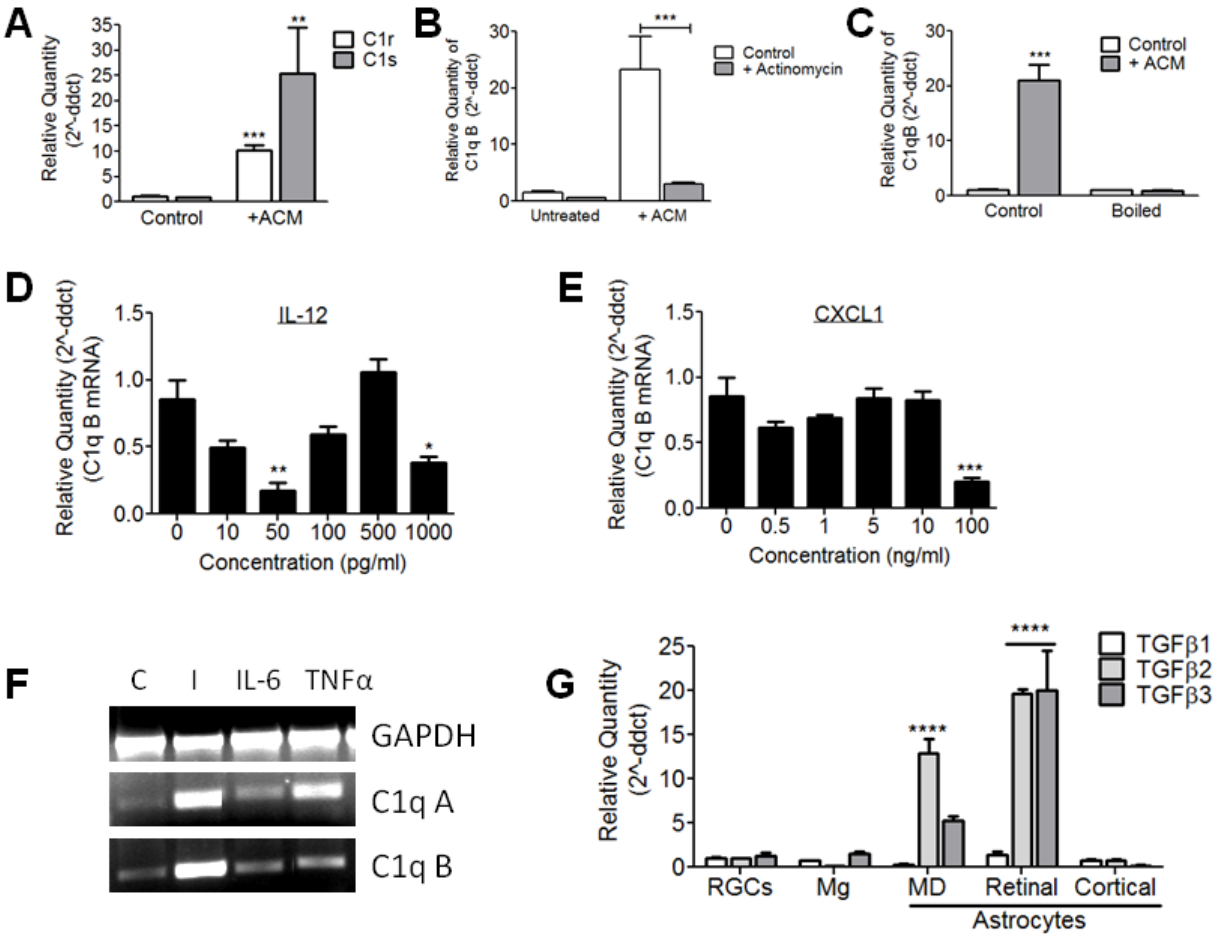

Supplemental Figure 1. In vitro characterization of cytokine or ACM-induced C1q upregulation. (A) *C1r* and *c1s*, the two genes that associate with C1q to form the C1 complex, are also significantly upregulated at 15 min by qPCR (one-way ANOVA, n=3 experiments, **p<0.01, ***p<0.001, F(1,8)=73.29). **(B)** A transcriptional inhibitor, actinomycin, blocks C1q upregulation, supporting that C1q upregulation is a transcriptional event (two-way ANOVA, n= 3 experiments, ***p<0.001, F(1,8)=4949.46). **(C)** Boiled ACM does not upregulate C1q, suggesting that a protein in ACM upregulates C1q (two-way ANOVA, n=3 experiments, ***p<0.001, F(1,8)=18.53). **(D)** IL-12 concentration response curve showed that RGCs did not upregulate C1q significantly (after 15 min. treatment) at any concentration tested (two-way ANOVA, n=3 samples per treatment, **p<0.01, *p<0.05, F(5,12)=14.75). **(E)** CXCL1 failed to upregulate C1q in RGCs (after 15 min. treatment) at any concentration tested (two-way ANOVA, n=3 samples per treatment, ***p<0.001, F(5,12)=11.06). **(F)** RT-PCR analysis of *c1qa* and *c1qb* expression shows a robust upregulation of C1q by insert (I) versus control (C), while IL-6 or TNFα treatment induces a modest increase in C1q. **(G)** TGF-β3 mRNA is enriched in retinal astrocytes compared to other astrocytes (McCarthy and de Vellis (MD) preparation and purified cortical astrocytes (cortical), RGCs, and microglia (Mg) (two-way ANOVA, n=3 experiments, ***p<0.001, F(8,45)=15.88).

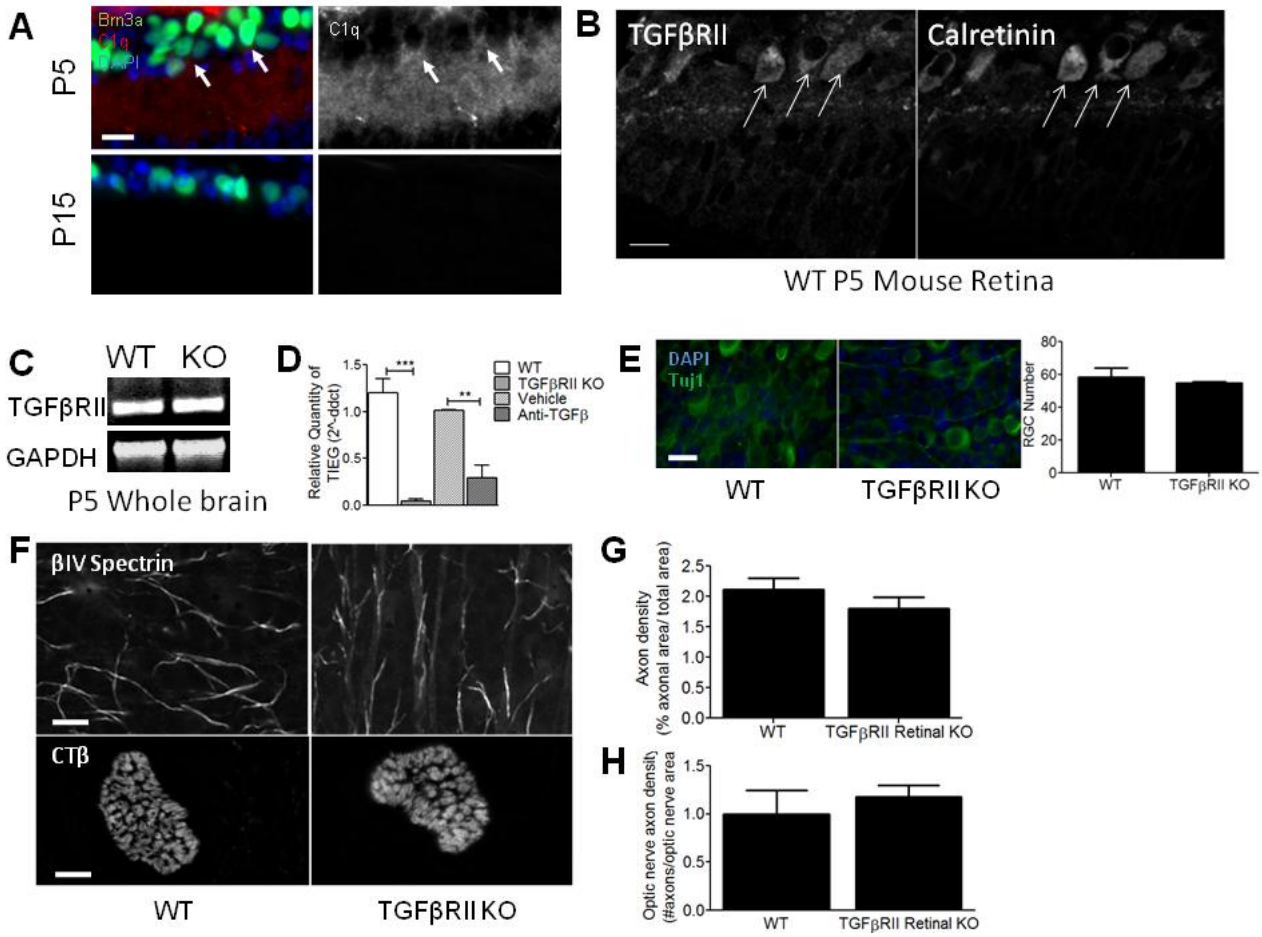

Supplemental Figure 2. Validation of retinal *TGFβRII*$^{-/-}$ mouse (A) C1q immunostaining is developmentally regulated in the IPL and RGC retinal layers. Scale bar = 20µm. **(B)** Co-localization of TGFβRII and calretinin by immunohistochemistry indicates that TGFβRII is expressed on RGCs *in vivo*. Scale bar = 20µm. **(C)** RT-PCR using RNA from P5 whole brain lysates from retinal *TGFβRII*$^{-/-}$ and WT littermates shows no difference in *tgfbr2* expression. **(D)** Validation that a known TGF-β-dependent gene, *TIEG*, is downregulated in the retinal *TGFβRII*$^{-/-}$ mouse and when anti-TGF-β is injected into the eye (one-way ANOVA, n=3 samples/group, **p<0.01, ***p<0.001, F(3,8)=27.93). **(E)** Whole mount retina immunostaining for Tuj1 shows no difference in the number of RGCs in TGFβRII retinal KO mice vs. WT littermates. (t test, n=4 mice/group, p=0.4040 no significance, t(6)=0.897539). Scale bar =30µm. **(F)** Immunohistochemistry with anti-βIV spectrin to mark axon initial segments showed similar numbers in WT and retinal *TGFβRII*$^{-/-}$ retinas. Scale bar = 30µm. Bottom panel: Axon density was measured by counting the number of fascicles (labeled by intraocular injection of CTB conjugated to Alexa 488) in the nerve/area of the optic nerve cross section. **(G)** Axon initial segment density was determined by measuring the area of axons/area of the field. Density was measures for 10 fields of view per mouse and normalized to WT (t test, n=3 mice, p=0.2993 (ns), t(4)=1.192). **(H)** Quantification of axon density showed no difference between WT and retinal *TGFβRII*$^{-/-}$ mice (t test, n=3 mice, p=0.5575 (ns), t(4)=0.6391).

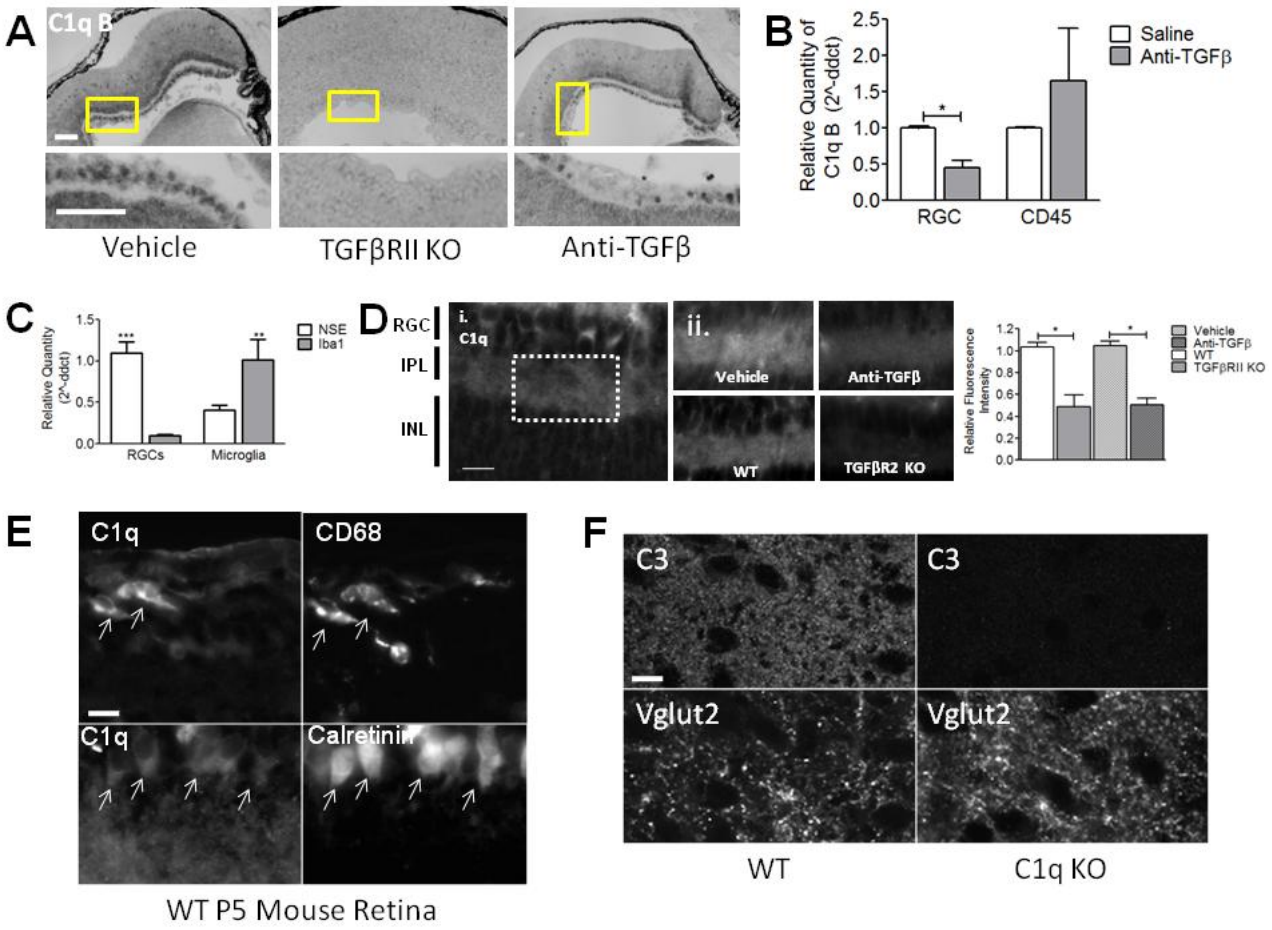

Supplemental Figure 3. Blocking TGF-β signaling with anti-TGF-β reduces C1q expression levels. (A) *In situ* for *c1qa* shows expression of C1q in the RGC layer is significantly reduced in the retinal *TGFβRII*$^{-/-}$ mouse and shows a patchy reduction in anti-TGF-β injected mice. Scale bar =100µm. **(B)** RGCs acutely isolated from P5 WT saline injected (white bar) and anti-TGF-β injected (grey bar) mouse retinas using immunopanning showed a significant reduction in C1q expression (two-way ANOVA, n= 4 mice/group, *p<0.05, F(2,18)=7.108). Microglia acutely isolated using CD45 immunopanning show no difference in C1q levels. **(C)** Acutely isolated RGCs and microglia were checked for the expression of neuron specific and microglia specific genes, *nse* and *iba1*, respectively. RGCs were significantly enriched for *nse* compared to microglia and microglia were significantly enriched for *iba1* compared to RGCs (two-way ANOVA, n=5 samples/group, **p<0.01,***p<0.001, F(1,16)=224.5). **(D)** Quantification of the relative fluorescence intensity in the IPL of anti-TGF-β injected and WT vehicle injected littermates shows a significant reduction in C1q localization to the IPL when TGF-β signaling is blocked (one-way ANOVA, n= 4 mice/group, *p<0.05, F(3,12)=6.306). Scale bar = 50µm. **(E)** Immunohistochemistry validation of C1q localization to RGCs and microglia as shown by C1q co-localization with markers for microglia (CD68) and RGCs (Calretinin). Co-localized cells indicated by arrows. Scale bar = 20µm. **(F)** Immunohistochemistry for C3 (Cappel, goat anti-C3) shows a reduction in C3 levels in the *C1q*$^{-/-}$ relative to WT littermate controls. Images shown are representative of 4 mice. Scale bar = 20µm.

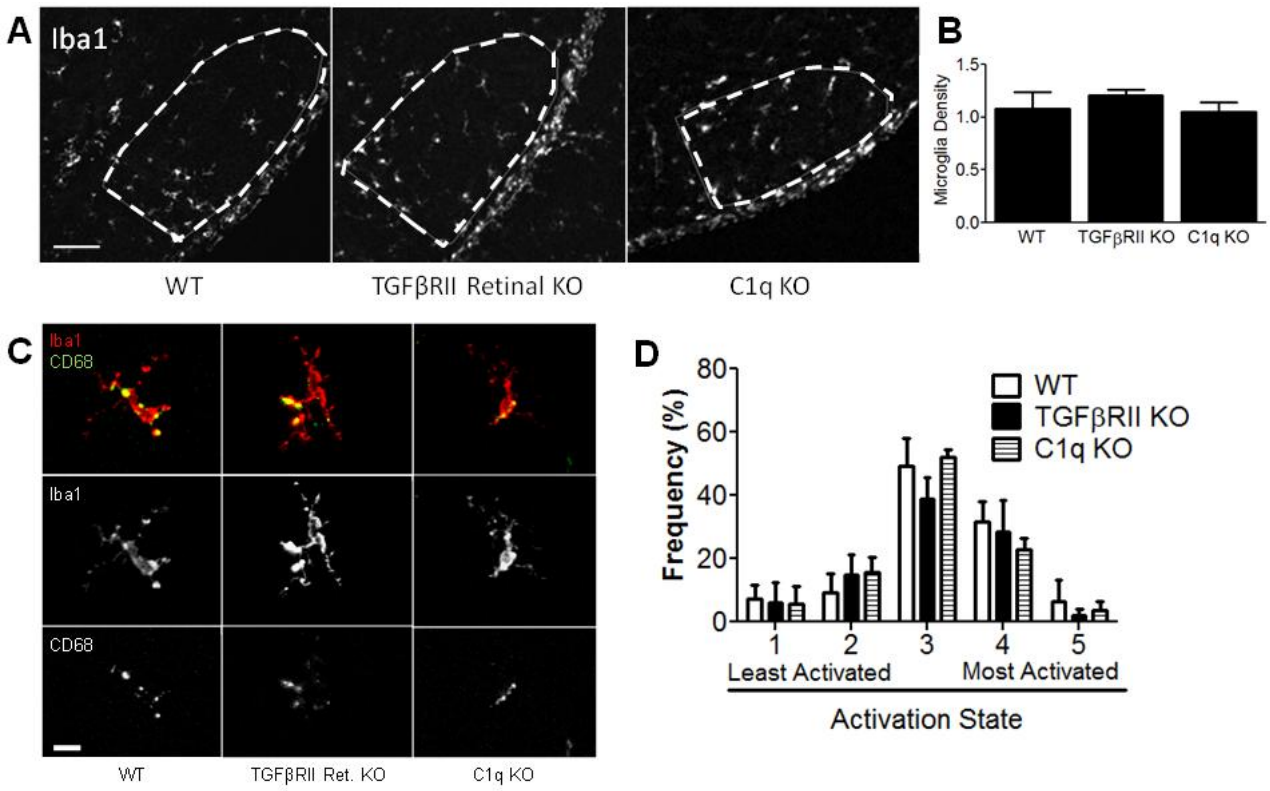

Supplemental Figure 4. Microglia numbers and localization are unaffected in TGFβRII retinal KO mice. (A) Representative images stained for Iba1 show that microglia morphology and distribution are similar in WT, retinal *TGFβRII*$^{-/-}$, and C1q$^{-/-}$ mice. Scale bar= 100µm. **(B)** Quantification of microglia density within the dLGN shows similar densities in WT, retinal *TGFβRII*$^{-/-}$, and C1q$^{-/-}$ mice (one-way ANOVA, n= 4 animals/group, p=0.7849 (ns), F(2,9)=0.2489). Density was calculated as the number of microglia divided by the dLGN area, excluding optic tract. Numbers were normalized to WT. **(C)** Representative microglia from P5 dLGN showed similar activation states in WT, retinal *TGFβRII*$^{-/-}$, and C1q$^{-/-}$ mice based on established activation state markers[7]. **(D)** WT, retinal *TGFβRII*$^{-/-}$, and C1q$^{-/-}$ mice showed a similar distribution of microglia activation state in the P5 dLGN. Microglia from two dLGN sections were sampled and immunostained for Iba1 (Dako) and CD68. (two-way ANOVA, n=4 mice/condition, p=0.6463 (ns), F(4,20)=0.63).

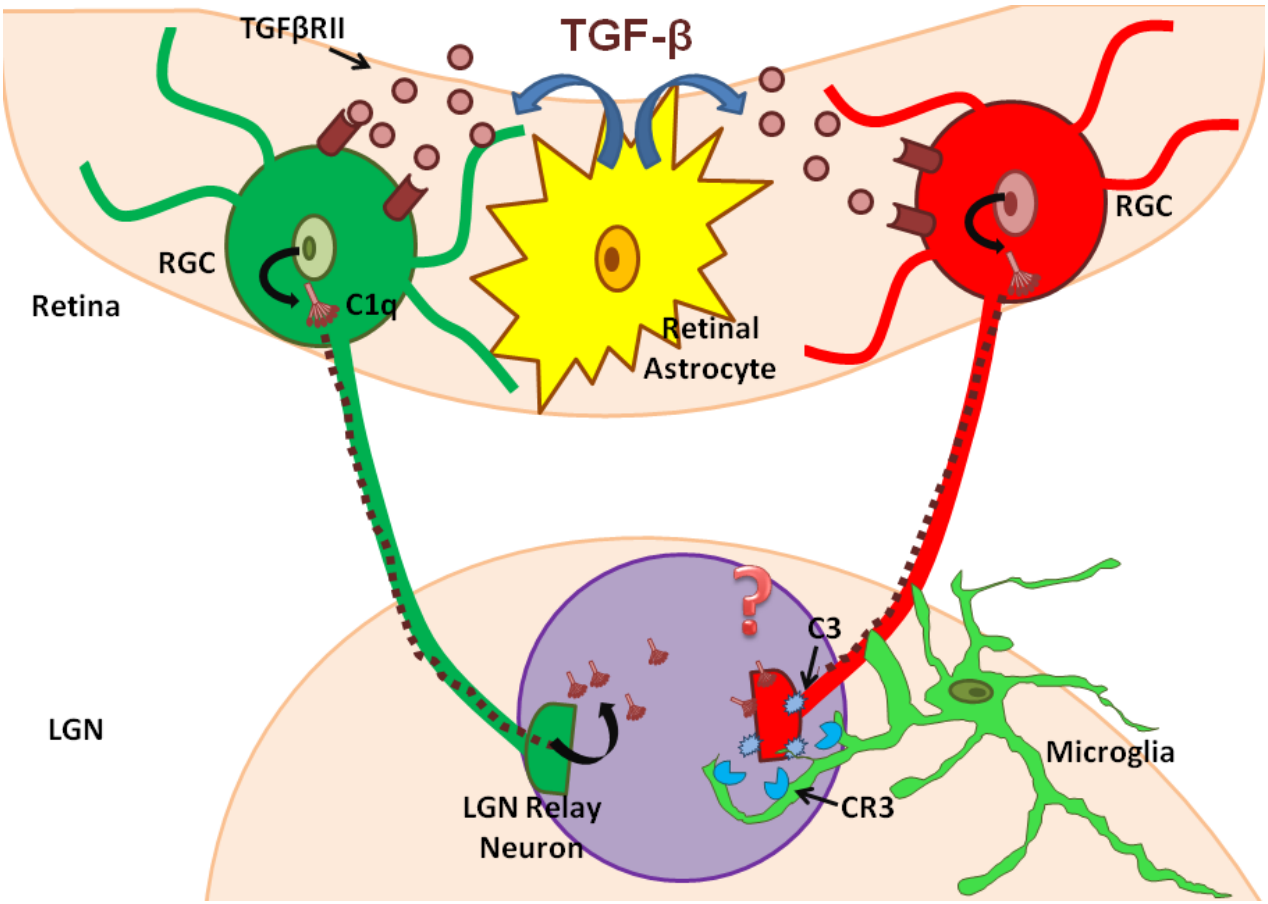

Supplemental Figure 5. Model of Complement-dependent Synapse Elimination. Our data and previous work support a model in which RGCs express C1q in response to TGF-β signaling and secrete C1q from their axon terminals in the dLGN. Once secreted, C1q localizes to inappropriate synapses where it triggers the classical complement cascade. C3 becomes activated and binds to inappropriate synapses, recruiting phagocytic microglia, expressing CR3, to remove inappropriate synapses by engulfment[7]. Microglia preferentially engulf less active retinogeniculate inputs (red axon)[7]; however it is not yet known whether or how complement targets weak inputs for elimination or if other mechanisms protect the specific (ie. stronger) synaptic inputs from elimination.

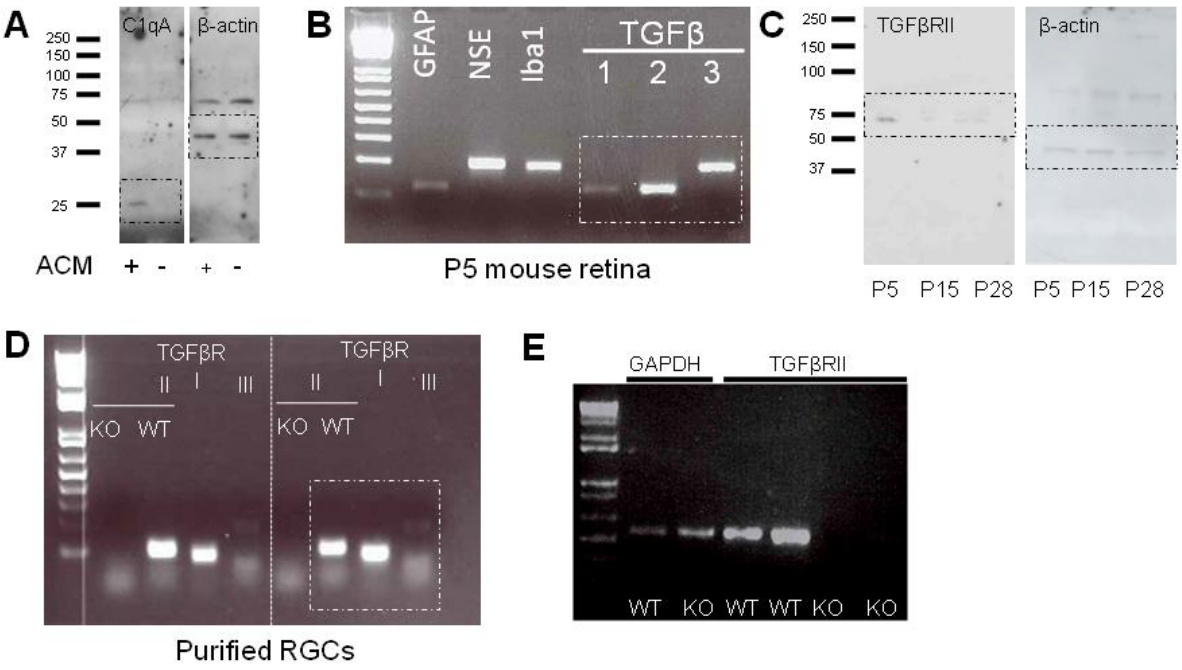

Supplemental Figure 6. Full-length pictures of the blots presented in the main figures. **(A)** Fig. 1d **(B)** Fig.3a **(C)** Fig. 3b **(D)** Fig. 2i **(E)** Fig. 3e